

## A comparison between coral colonies of the genus *Madracis* and simulated forms

Maxim V. Filatov, Jaap A. Kaandorp, Marten Postma, Robert van Liere, Kris J. Kruszynski, Mark J. A. Vermeij, Geert J. Streekstra and Rolf P. M. Bak

*Proc. R. Soc. B* published online 23 June 2010  
doi: 10.1098/rspb.2010.0957

---

### Supplementary data

"Data Supplement"

<http://rsob.royalsocietypublishing.org/content/suppl/2010/06/22/rspb.2010.0957.DC1.html>

### References

**This article cites 18 articles, 1 of which can be accessed free**

<http://rsob.royalsocietypublishing.org/content/early/2010/06/22/rspb.2010.0957.full.html#ref-list-1>

### P<P

Published online 23 June 2010 in advance of the print journal.

### Subject collections

Articles on similar topics can be found in the following collections

[systems biology](#) (150 articles)  
[biomechanics](#) (142 articles)  
[ecology](#) (1821 articles)

### Email alerting service

Receive free email alerts when new articles cite this article - sign up in the box at the top right-hand corner of the article or click [here](#)

---

Advance online articles have been peer reviewed and accepted for publication but have not yet appeared in the paper journal (edited, typeset versions may be posted when available prior to final publication). Advance online articles are citable and establish publication priority; they are indexed by PubMed from initial publication. Citations to Advance online articles must include the digital object identifier (DOIs) and date of initial publication.

---

To subscribe to *Proc. R. Soc. B* go to: <http://rsob.royalsocietypublishing.org/subscriptions>

---

# A comparison between coral colonies of the genus *Madracis* and simulated forms

Maxim V. Filatov<sup>1</sup>, Jaap A. Kaandorp<sup>1,\*</sup>, Marten Postma<sup>1</sup>,  
Robert van Liere<sup>2</sup>, Kris J. Kruszyński<sup>2</sup>, Mark J. A. Vermeij<sup>3,4</sup>,  
Geert J. Streekstra<sup>5</sup> and Rolf P. M. Bak<sup>6</sup>

<sup>1</sup>Section Computational Science, Faculty of Science, University of Amsterdam, Science Park 107,  
1098 XG Amsterdam, The Netherlands

<sup>2</sup>Center for Mathematics and Computer Science, Kruislaan 413, 1098 Sĳ Amsterdam, The Netherlands

<sup>3</sup>Carmabi Foundation, Piscaderabaai z/n, Curaçao, Netherlands Antilles

<sup>4</sup>IBED, University of Amsterdam, Nieuwe Achtergracht 127, 1018 WS Amsterdam, The Netherlands

<sup>5</sup>Academic Medical Center, Department of Biomedical Engineering and Physics, Meibergdreef 9,  
1105 AZ Amsterdam, The Netherlands

<sup>6</sup>Department of Marine Ecology, Netherlands Institute of Sea Research (NIOZ), PO Box 59,  
1790 AB Den Burg, The Netherlands

In addition to experimental studies, computational models provide valuable information about colony development in scleractinian corals. Using our simulation model, we show how environmental factors such as nutrient distribution and light availability affect growth patterns of coral colonies. To compare the simulated coral growth forms with those of real coral colonies, we quantitatively compared our modelling results with coral colonies of the morphologically variable Caribbean coral genus *Madracis*. *Madracis* species encompass a relatively large morphological variation in colony morphology and hence represent a suitable genus to compare, for the first time, simulated and real coral growth forms in three dimensions using a quantitative approach. This quantitative analysis of three-dimensional growth forms is based on a number of morphometric parameters (such as branch thickness, branch spacing, etc.). Our results show that simulated coral morphologies share several morphological features with real coral colonies (*M. mirabilis*, *M. decactis*, *M. formosa* and *M. carmabi*). A significant correlation was found between branch thickness and branch spacing for both real and simulated growth forms. Our present model is able to partly capture the morphological variation in closely related and morphologically variable coral species of the genus *Madracis*.

**Keywords:** corals; morphogenesis; morphology; simulation; CT scan; *Madracis*

## 1. INTRODUCTION

Scleractinian corals exhibit great inter- and intraspecific variation in coral colony morphology (e.g. Veron 1995; Bruno & Edmunds 1997). Intra-specific variation often arises from plasticity in a colony's growth process in response to variable environmental conditions, such as flow speed, availability of light and availability of dissolved inorganic carbon (Muko *et al.* 2000; Todd *et al.* 2004; Todd 2008). Because genetic and environmental factors determine a colony's three-dimensional structure, the relative importance of either factor is often difficult to determine. Experimental studies whereby corals are grown under different environmental conditions are often limited by the slow growth rates of corals and difficulties with controlling environmental parameters of the system. Therefore, plastic responses to environmental changes are studied in relatively few (about 17) coral species (Todd 2008).

To determine the degree of phenotypic plasticity among colonies of the same species under variable environmental conditions, various morphometric traits

are measured to quantitatively assess whether changes in coral colony growth and form correlate with varying environmental factors (e.g. Bruno & Edmunds 1997). Morphological variation in corals exists on different scales, from differences in corallite structure within a single colony (Foster 1979) to variation among colonies in a single species. The present study aims to describe variability at the colony morphology level in species of the Caribbean coral genus *Madracis*. The *Madracis* species are characterized by the encrusting (*M. pharensis*), nodular (*M. decactis*) or branching colonies (*M. formosa*, *M. mirabilis*, *M. carmabi*; Wells 1973a,b; Fenner 1993; Vermeij *et al.* 2003). Morphological traits such as the branch diameter and branch spacing in *M. mirabilis* are under the influence of the environment (Bruno & Edmunds 1997). Other corals, such as *Stylophora pistilata* and *Acropora eurystroma*, also tend to have a certain degree of phenotypic plasticity (Borgiorni *et al.* 2003; Shaish *et al.* 2007). Some corals, on the other hand, show very little or no phenotypic response to environment (e.g. *Pavona cactus*; Willis 1985), suggesting that in this species colony morphology is primarily driven by genetic factors.

Computational models support the evidence of phenotypic plasticity found in biological experiments. The amount of light and nutrient distribution have been

\* Author for correspondence (j.a.kaandorp@uva.nl).

Electronic supplementary material is available at <http://dx.doi.org/10.1098/rsob.2010.0957> or via <http://rsob.royalsocietypublishing.org>.

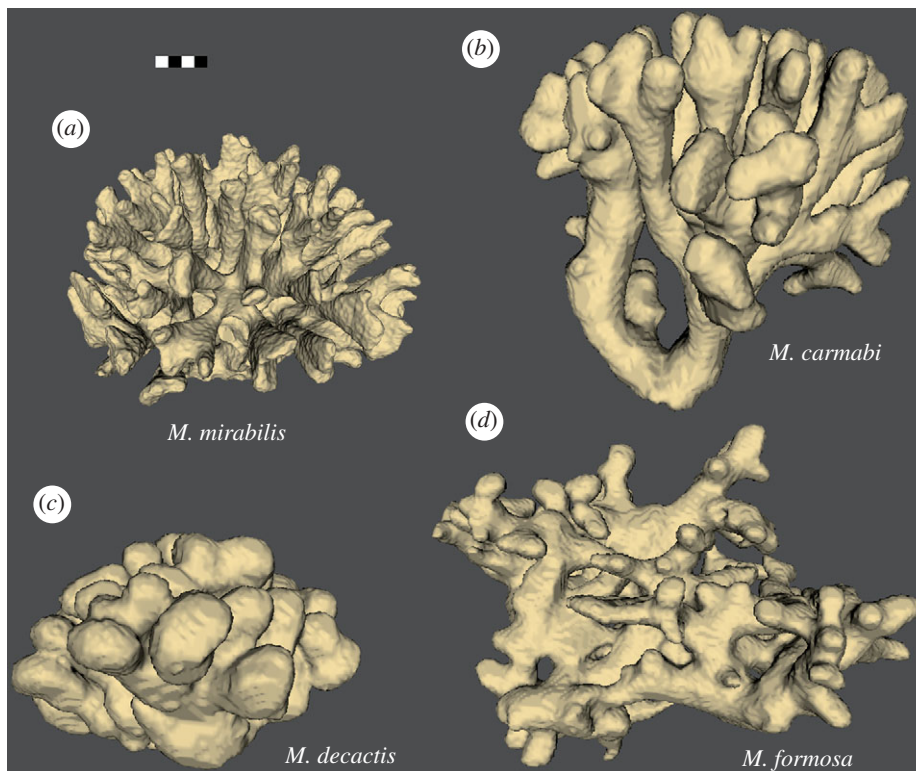


Figure 1. Volume rendering of the CT scans of real coral colonies (scale bar, 2 cm).

used to simulate a range of coral morphologies under different environmental conditions (Graus & MacIntyre 1982; Muko *et al.* 2000; Kaandorp & Kübler 2001; Merks *et al.* 2004; Kaandorp *et al.* 2005). Using a computational approach, Kaandorp *et al.* (2005) found that gradients in dissolved inorganic carbon (DIC) around coral colonies are responsible for branching colony morphologies. A field experiment to investigate the same phenomenon would be practically impossible due to the slow growth of colonies in the field and problems associated with measuring DIC at the sub-millimetre scale as used in the computational study. Therefore, in addition to field experiments, computational models are an important alternative to study processes at very different time and spatial scales.

Here, we validate the previously developed coral growth model (Merks *et al.* 2004), which combines the effects of variable environmental parameters with variation in species-specific information (i.e. distance between polyps and polyp height; Kaandorp *et al.* 2005). We compare the modelling results with colonies of different *Madracis* species. The model is suitable for simulating corals that have non-polymorphic polyps (e.g. *Madracis* species), since there is no differentiation in axial and radial polyps in *M. mirabilis* colonies. This contrasts with, for example, *Acropora* species, where a fast growing axial polyp occurs at the tip of each branch (Wallace 1999), which differs from the other (radial) polyps on the same branch. The simulations produced by the growth model produce morphologies that resemble the shape of coral colonies belonging to the Caribbean coral species *M. mirabilis* (figure 1*a*). In general, objects generated by the model can be characterized by very regular branch spacing. This makes them suitable for comparison with real colonies of *M. mirabilis* (figure 1*a*) that show similar regular branch spacing.

Verification of the model by quantitative comparison of colony morphologies between simulation results and real coral colonies is crucial for further exploration of factors involved in coral colony development. For a comparative analysis, we can use quantitative measurements of such morphological traits as branch spacing, branch thickness, branching angle and branching rate of real coral colonies and simulated growth forms. A recently developed morphometric method is using high resolution computed tomography (CT) scans of coral colonies to provide such information (Kruszynski *et al.* 2007). In the present study, a quantitative morphological analysis is applied to a range of simulated morphologies and to CT scans of real colonies of several coral species belonging to the genus *Madracis*, namely *M. decactis*, *M. carmabi*, *M. formosa* and *M. mirabilis*. The relation between several morphological traits of the coral colonies will be investigated. This quantitative approach allows for classification of the coral morphologies based on the shape of the colony. We will demonstrate that coral morphologies can be classified using a set of morphometric traits.

## 2. MATERIAL AND METHODS

### (a) Data acquisition

*M. mirabilis* ( $n = 3$ ), *M. carmabi* ( $n = 10$ ), *M. decactis* ( $n = 10$ ) and *M. formosa* ( $n = 7$ ) colonies were collected at depths between 6 and 50 m on Curaçao (Netherlands Antilles, 12° N, 69° W). Three-dimensional images of these colonies were obtained using CT scanning techniques (Kaandorp & Kübler 2001). The CT scans were made at a resolution with a voxel (i.e. volumetric pixel) size of  $0.33 \times 0.33 \times 1.50$  mm (*M. carmabi*, *M. decactis* and *M. formosa*) and almost isotropic voxel size of  $0.25 \times 0.25 \times 0.30$  mm (*M. mirabilis*). The number of slices per colony varies between 45 and 765, depending on overall colony size. The

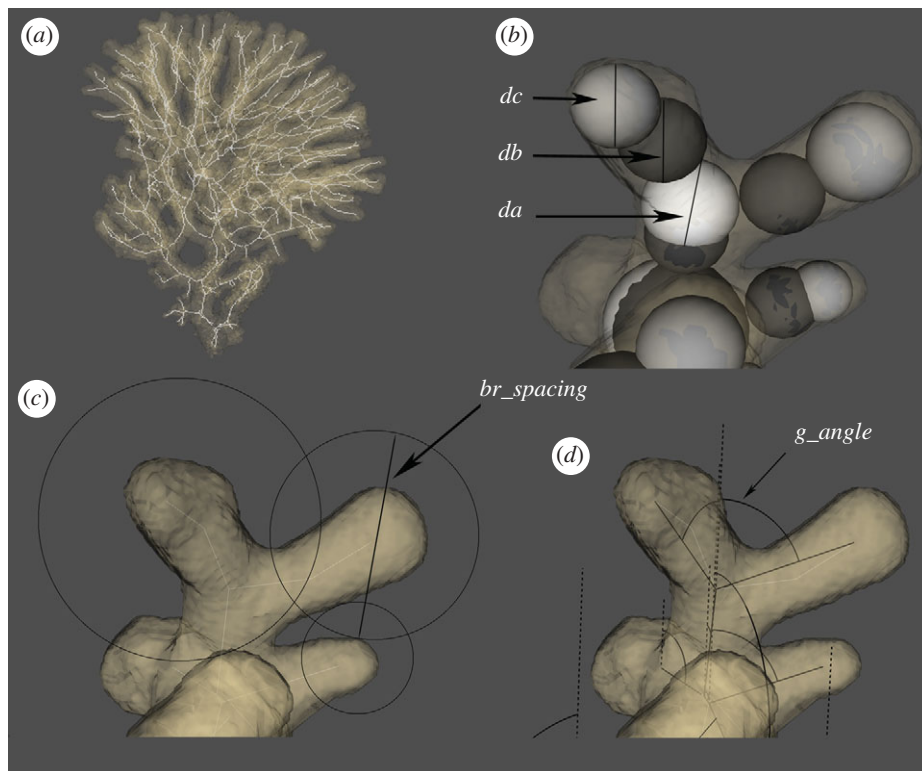


Figure 2. (a) Morphological skeleton generated from a volume, (b) branch thickness ( $da$ , white sphere;  $db$ , black sphere;  $dc$ , grey sphere), (c) branch spacing ( $br\_spacing$ ) and (d) branching angle relative to the growth direction ( $g\_angle$ ).

three-dimensional data were edited (the substrate plate on which samples were lying was cropped) and visualized using the open source OSIRIX imaging software. In figure 1, these datasets are visualized using volume rendering. Three-dimensional objects generated by three-dimensional surface rendering are used for the morphometric analyses described below.

### (b) Morphometrics

By using CT scans in morphometric software (Kruszynski *et al.* 2007), some of the key morphometric features of the coral colonies can be measured. Morphometric analyses start with the construction of a morphological skeleton of each three-dimensional object, which consists of the medial axis of each branch, shown in figure 2a. This is done by the skeletonization algorithm described in Kruszynski *et al.* (2007).

By combining volumetric information and the morphological skeleton derived from the medial axis it is possible to measure the following morphological parameters. Branch thickness at the beginning of a branching point is defined by the diameter ( $da$ ) of the white sphere in figure 2b. The diameter ( $db$ ) of the black sphere (figure 2b) defines the branch thickness after branching. The diameter ( $dc$ ) of the grey sphere located at the endpoint of a branch defines the thickness of a branch tip. Branching angle ( $b\_angle$ ) is measured between the lines connecting centre points of the  $a$ -sphere (white) and  $b$ -sphere (black). Branching angle relative to the growth direction ( $g\_angle$ ) is measured between the positive  $y$ -axis and a branch (figure 2d). Branching rate ( $rb$ ) is defined as the length of the edge connecting two successive  $a$ -spheres. Branch spacing ( $br\_spacing$ ) is equal to the radius of a sphere centred at the branch tip, which reaches the closest branch (figure 2c). The same morphological features were measured in simulated objects to allow a comparison of these parameters between simulated and real coral

colonies. More detailed information about the algorithms used by the morphometric software can be found in Kruszynski *et al.* (2007).

### (c) Simulations with the accretive growth model

An accretive growth model was used to simulate coral morphologies (Merks *et al.* 2004; Kaandorp *et al.* 2005). The model simulates the growth of the colony skeleton as an accretive process whereby subsequent growth layers are deposited on top of the previous one as the coral colony grows. The geometry of each layer is represented by a triangulated surface. The distance  $l$  between the two layers (i.e. skeleton thickness) is assumed to be linearly dependent on the amount of absorbed nutrients and local light intensity:

$$l = (1 - \alpha)\bar{n}c_i^{\text{nutrient}} + \alpha c_i^{\text{light}}, \quad 0 \leq \alpha \leq 1, \quad (2.1)$$

where  $\bar{n}$  denotes the average normal at vertex  $i$ ,  $c_i$  denotes the amount of absorbed nutrients or light, and  $\alpha$  denotes the parameter controlling relative contribution of light intensity and nutrient concentration to the growth process.

The main assumption made in the model is that the growth of the skeleton is limited by the amount of local availability of DIC and light in the environment. Higher DIC availability promotes calcification, depending on light availability (Gattuso *et al.* 1999). Branching in the simulated object emerges from competition between the polyps for available nutrients (Merks *et al.* 2004).

The simulation occurs within a three-dimensional volume (i.e. simulation box; figure 3). As an initial object, a sphere is placed in the middle of the volume on the bottom plane. Simulated DIC propagates through the volume by means of diffusion. The top plane of the simulation box acts as source, and the bottom plane and the surface of the simulated object as a sink for nutrients. The diffusion is modelled using

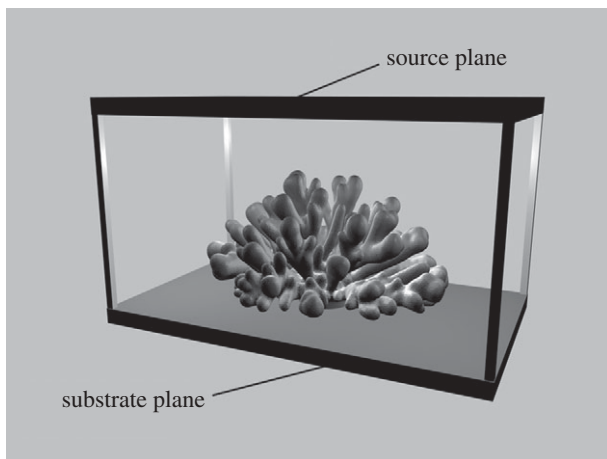


Figure 3. Simulation set-up. A growing object bounded by the simulation box with a source plane on the top and the substrate plane at the bottom.

the lattice Boltzmann method (Chopard & Droz 1998; Succi 2001). The nutrient distribution is recomputed after each growth step of the simulated object. Different boundary conditions can be applied: nutrient source at the top plane or additional nutrient source from all four side planes. These conditions were assumed to represent situations whereby the nutrient supply towards an isolated, simulated colony occurs with or without competition from neighbouring colonies, respectively.

The model uses several species-specific parameters such as distance between polyps and polyp height. The latter is modelled by the absorption of nutrients at a short distance from the skeleton surface. By varying environmental modelling parameters such as light intensity, nutrient availability and the degree of diffusion of the nutrients across the object surface, we simulate various morphologies. The translocation of absorbed nutrients between the neighbouring polyps is modelled by lateral diffusion across the surface of the object,

$$\frac{\partial c(x, t)}{\partial t} = D\nabla^2 c(x, t), \quad (2.2)$$

where  $c$  is the concentration of nutrients at point  $x$ ,  $t$  the time and  $D$  the diffusion coefficient.

#### (d) Measurements

The quantification of the morphometric parameters of the simulated corals and CT scans is presented as a series of histograms (see the electronic supplementary material). Every branch, branching angle and other features are measured for each colony resulting in a large number (order of 100) of measurements per colony. For each colony a distribution of each measured morphological trait (e.g. branch thickness) is calculated. Subsequent morphological analysis is carried out based on these distributions.

#### (e) Statistical analysis

Data were normalized to allow the comparison of dimensionless descriptors of real and simulated coral morphologies. Additionally, outliers were removed using the extreme studentized deviate (ESD) many-outlier procedure ( $k = 3$ ,  $\alpha = 0.05$ ; Rosner 1983). Correlation analyses were used to detect relationships among the descriptors of colonies' morphological traits. The correlation matrix between all measured parameters and corresponding  $p$ -values can be found in the electronic supplementary material. Scatter plots for all pairs

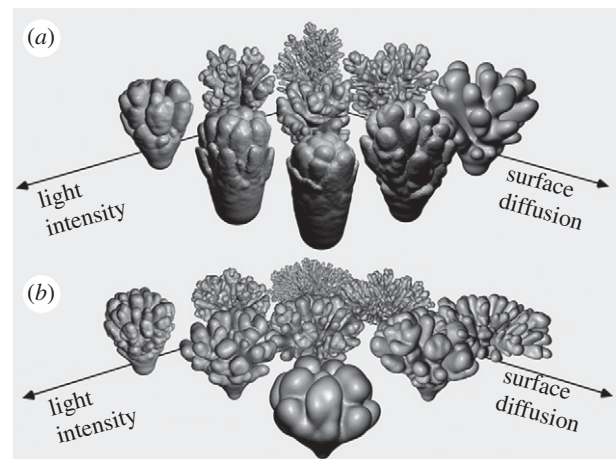


Figure 4. Morphospace of simulated coral colonies in two different environments: (a) nutrient source is above the object (i.e. mimicking the presence of competing colonies near the simulated colony); (b) side planes act also as the nutrient source (i.e. mimicking the absence of competing colonies near the simulated colony). The axes represent parameters that can be gradually changed in order to change colony morphology. Light intensity is the  $\alpha$  parameter from equation (2.1). Surface diffusion is the diffusion constant  $D$  in equation (2.2).

of variables are presented in the electronic supplementary material, figure SA.3. For comparison between real and simulated coral morphologies we use multivariate data analyses. We carried out principal component analysis (PCA), discriminant analysis (DA) and multivariate analysis of variance (MANOVA) methods on normalized variables. DA was used to classify samples with quadratic discriminant function. Multi-dimensional scaling (MDS) was also applied on the distance matrix to visualize dissimilarities between the samples in the Euclidean two-dimensional space.

### 3. RESULTS

The range of simulated coral morphologies in response to interacting levels of light and nutrient diffusion across the coral colony's surface is given in figure 4. By gradually increasing the values of two model parameters for light intensity and surface diffusion, thin-branched morphologies are transformed into more compact growth forms.

A complete overview of all measured morphological traits of the simulations and real coral colonies can be found in the electronic supplementary material, A.8 histograms. We found three significantly ( $p < 0.0001$ ) correlated variables in both simulated and real shapes. The strongest linear correlation ( $r = 0.73$ ,  $p < 0.0001$ ) was observed between branch spacing ( $br\_spacing$ ) and branching rate ( $rb$ ). Branching rate ( $rb$ ) is also correlated ( $r = 0.68$ ,  $p < 0.0001$ ) with branch thickness ( $db$ ). In addition to linear correlation ( $r = 0.67$ ,  $p < 0.0001$ ) between branch thickness ( $db$ ) and branch spacing ( $br\_spacing$ ), a scatter plot of these two variables (figure 5) shows that species tend to group more among each other than with colonies of other species. Scatter plots and correlation coefficients of all other variables can be found in the electronic supplementary material, A3.

Morphological variation is illustrated using a PCA scatter plot for the first two principal components (PC1

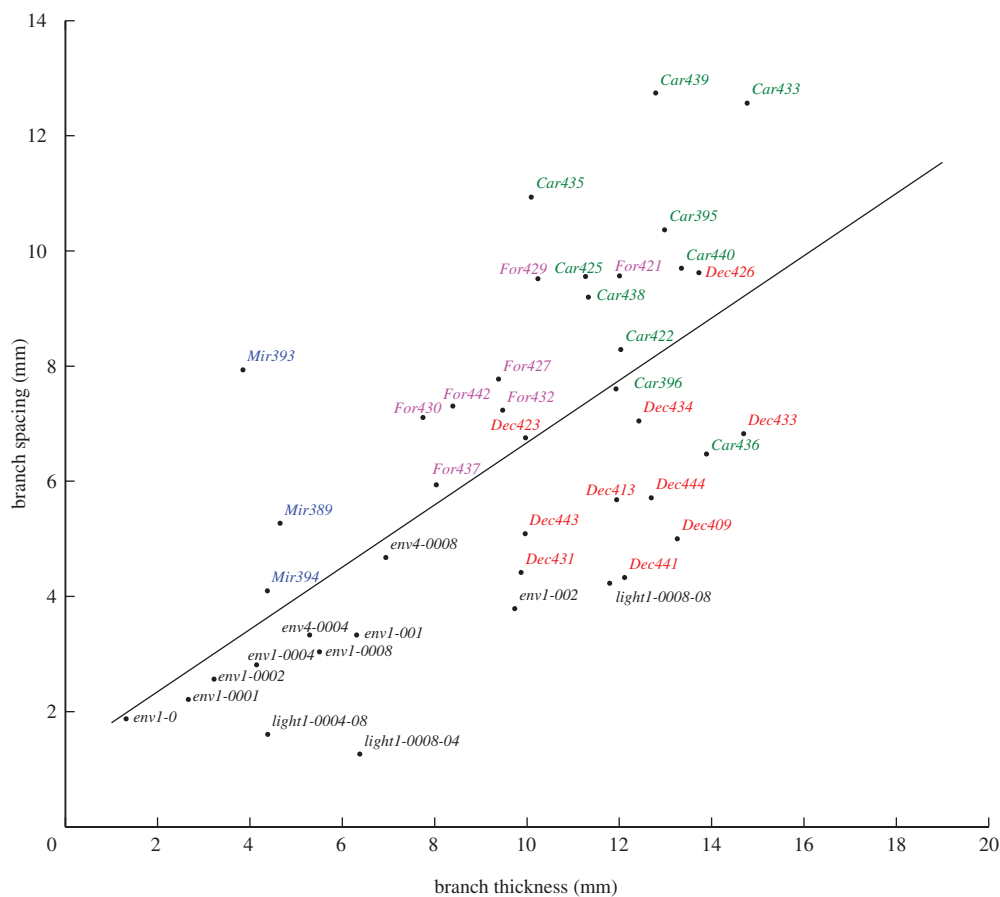


Figure 5. A scatter plot of the correlation between branch thickness ( $db$ ) and branch spacing ( $br\_spacing$ ). In coloured labels of real corals the first three characters denote the name of the species (i.e. *Mir* = *M. mirabilis*, *For* = *M. formosa*, *Dec* = *M. decactis* and *Car* = *M. carmabi*), followed by the identification number in our coral database. Simulated growth forms are denoted using black labels, where the simulated environment ( $env1$  = one source plane or  $env4$  = four additional source planes) is followed by the value of surface diffusion coefficient. In simulations where the influence of light is taken into account ( $light1$ ) the value of the surface diffusion coefficient is followed by the value of the light intensity parameter.

and PC2; figure 6). The simulations and *M. mirabilis* species are mostly distinguished from the other species by the first principal component. PC1 and PC2 together describe 68 per cent of variance in the dataset. Other principal components are not sufficient for the discrimination of the samples. A DA applied to the first two PCs shows the classification of the species and simulations (see the electronic supplementary material, A6).

By testing different subsets of variables we found that three morphological traits are most suitable to discriminate between different coral species: the thickness in the middle of the branch ( $db$ ), branch spacing ( $br\_spacing$ ) and the ratio  $da/rb$ . A visualization of this parameter space with MDS is presented in the electronic supplementary material, figure SA.5.

The significance of the dissimilarities between the species (including simulations) was analysed using MANOVA. In this analysis five groups were compared: (i) *M. mirabilis*; (ii) *M. decactis*; (iii) *M. carmabi*; (iv) *M. formosa*; (v) simulations. The number of dimensions containing group means was  $d = 2$  ( $\alpha = 1\%$ ,  $p < 0.001$ , Wilk's  $\lambda = 0.022$ ). Therefore, we used the first two canonical vectors (CVs) to visualize the results. The MANOVA plot of the first two CVs is presented in figure 7. Simulations form a close group with two outliers ( $env1-0$  and  $env1-002$ ). Real corals (except for *M. mirabilis*) form a group with *M. formosa* in the middle

and *M. carmabi* and *M. decactis* on the separate ends of the group. *M. mirabilis* lies between the simulations and other coral species. The group that lies the closest to the simulations is *M. mirabilis*. A DA applied to the first two CVs shows the classification of the species and simulations (see the electronic supplementary material, A7).

#### 4. DISCUSSION

The comparative morphological analysis between simulations and real coral colonies shows that simulated forms share three morphological features with *Madracis* species described in this paper. Branch thickness ( $db$ ), branching rate ( $rb$ ) and branch spacing ( $br\_spacing$ ) are the basic traits that describe morphology of the branching shapes. Positive correlations between these traits show that in all species in this study the compactness of the colony is preserved. The same relationships between morphological features are also observed in the simulated forms. This supports assumptions made in our computational model that gradients of DIC and light availability in the direct environment of the colony play an important role in the shaping of corals (Merks *et al.* 2004; Kaandorp *et al.* 2005).

In figure 5, samples of the same species group together, with few outliers (e.g. *Car436*, *Dec426*, *For421*). However, a better discrimination between the species can be made

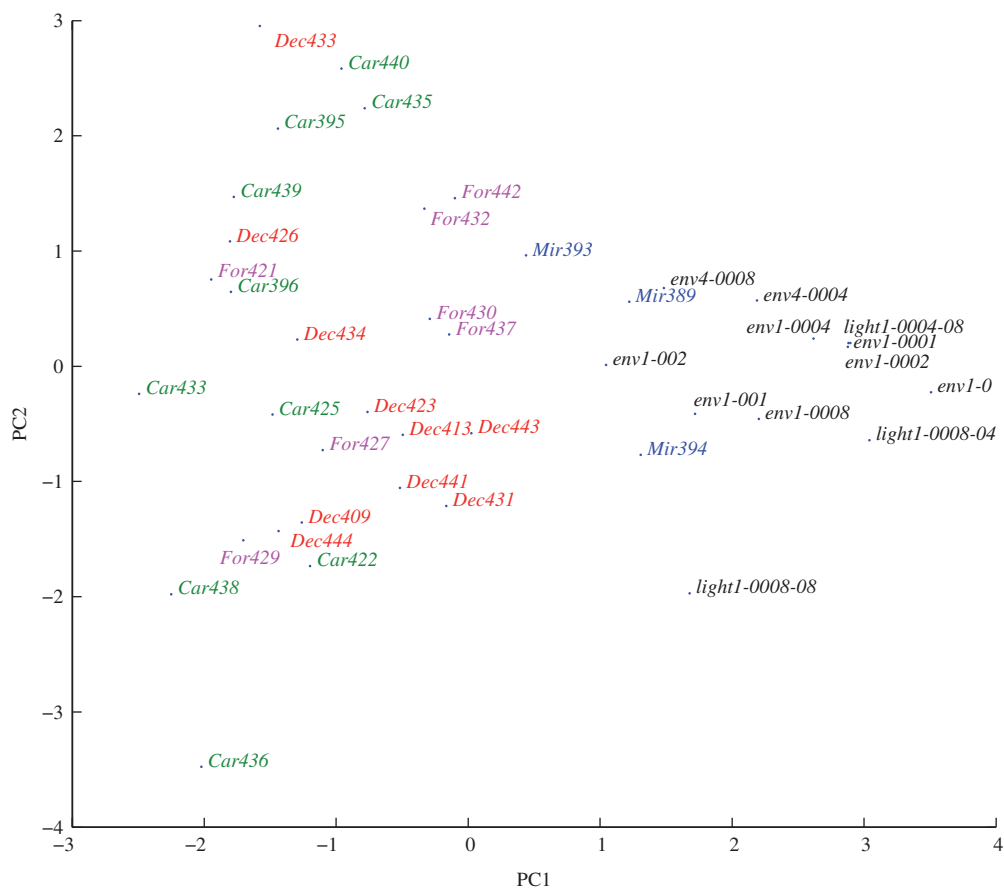


Figure 6. Scatter plot of the first two principal components. For the description of labels see caption of figure 5.

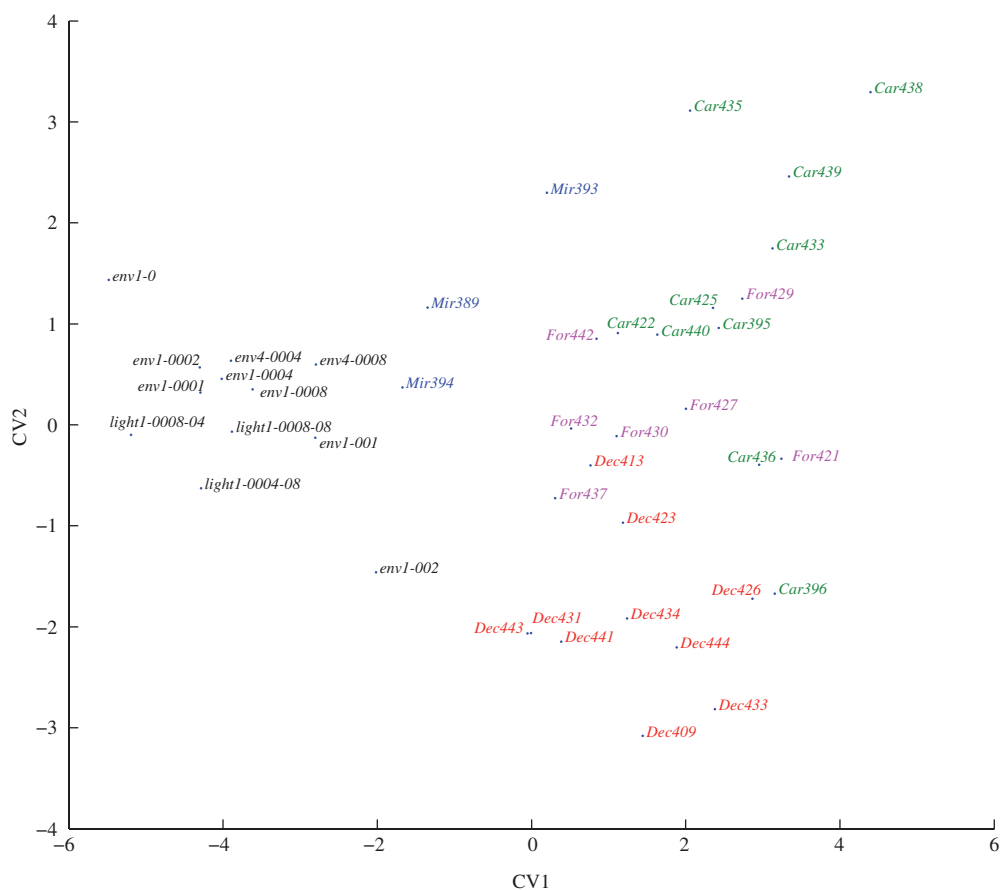


Figure 7. MANOVA plot of the first two canonical vectors (CVs). For the description of labels see caption of figure 5.

using multivariate analysis. In the MANOVA plot in figure 7, we can distinguish two groups: one group is the simulations and the second group consists of the three species *M. carmabi*, *M. decactis* and *M. formosa*. *Madracis mirabilis* lies closer to the simulations except for one sample (*Mir393*). This can be explained by the regular branching pattern of this species. The regularity of the branching patterns is measured by the standard deviation of the branch spacing (*br\_spacing*); see histograms in the electronic supplementary material. A lower value of the standard deviation indicates a higher regularity. We inspected the linear combinations of variables that form the first two CVs in the multi-variate analysis (MANOVA). Variables that contributed the most to these vectors were branch thickness (*db*), branching angle (*b\_angle*) and branch spacing (*br\_spacing*). Therefore, these morphological traits differ the most across the species and simulations.

The quantitative validation of our coral growth model demonstrates its ability to simulate a certain group of real corals. The simulated morphologies approximate the morphology of *M. mirabilis* colonies (electronic supplementary material, figure A.7), confirming an earlier study that compared simulated and coral colonies qualitatively (Kaandorp *et al.* 2005). However, the accretive growth model in its present state is not sufficient to simulate all colony morphologies of the *Madracis* species shown in this analysis. For instance, such morphologies as that of *M. formosa* in figure 1*d*, cannot be generated because of its irregular branching pattern. Some thick branched simulations (*env1-002* in figure 7) also resemble the morphology of *M. decactis* colonies.

Among model parameters there are two important environmental factors (i.e. light intensity and nutrient source distribution) and one intrinsic factor (nutrient surface redistribution). These factors are known to have an effect on a coral colony morphology (Todd 2008). Hydrodynamics, the structure of individual corallites and interpolyp communication are not modelled in the present study. Nevertheless, the present study has shown that basic principles of the coral colony morphogenesis can be captured in a computational model. The demonstrated range of simulated shapes (figure 4) can be significantly extended in at least two additional dimensions: first, by incorporating hydrodynamics into the model; and second, by adding physiological or genetic factors that will regulate the growth of a colony from within.

This work was funded by the Netherlands Organization for Scientific Research (NWO), VIEW project (no. 643100601).

## REFERENCES

- Borgiorni, L., Shafir, S., Angel, D. & Rinkevich, B. 2003 Survival, growth and gonad development of two hermatypic corals subjected to *in situ* fish-farm nutrient enrichment. *Mar. Ecol. Progr. Ser.* **253**, 137–144.
- Bruno, J. F. & Edmunds, P. J. 1997 Clonal variation for phenotypic plasticity in the coral *Madracis mirabilis*. *Ecology* **78**, 2177–2190.
- Chopard, B. & Droz, M. 1998 *Cellular automata modeling of physical systems*. Cambridge, UK: Cambridge University Press.
- Fenner, D. P. 1993 Species distinctions among several Caribbean stony corals. *Bull. Mar. Sci.* **53**, 1099–1116.
- Foster, A. B. 1979 Phenotypic plasticity in the reef corals *Montastrea annularis* and *Siderastrea siderea*. *J. Exp. Mar. Biol. Ecol.* **39**, 25–54. (doi:10.1016/0022-0981(79)90003-0)
- Gattuso, J.-P., Allemand, D. & Frankignoulle, M. 1999 Photosynthesis and calcification at cellular, organismal and community levels in coral reefs: a review on interactions and control by carbonate chemistry. *American Zoologist* **39**, 160–183.
- Graus, R. R. & Macintyre, I. G. 1982 Variation in growth forms of the reef coral *Montastrea annularis* (Ellis and Solander): a quantitative evaluation of growth response to light distribution using computer simulation. *Smithson. Contr. Mar. Sci.* **12**, 441–464.
- Kaandorp, J. A. & Kübler, J. E. 2001 The algorithmic beauty of seaweeds, sponges and corals. *Marine Biology*. Heidelberg, Germany: Springer.
- Kaandorp, J. A., Sloot, P. M. A., Merks, R. M. H., Bak, R. P. M., Vermeij, M. J. A. & Maier, C. 2005 Morphogenesis of the branching reef coral *Madracis mirabilis*. *Proc. R. Soc. B* **272**, 127–133. (doi:10.1098/rspb.2004.2934)
- Kruszynski, K. J., Kaandorp, J. A. & van Liere, R. 2007 A computational method for quantifying morphological variation in scleractinian corals. *Coral Reefs* **26**, 831–840. (doi:10.1007/s00338-007-0270-6)
- Merks, R. M. H., Hoekstra, A. G., Kaandorp, J. K. & Sloot, P. M. A. 2004 Polyp oriented modelling of coral growth. *J. Theor. Biol.* **228**, 559–576. (doi:10.1016/j.jtbi.2004.02.020)
- Muko, S., Kawasaki, K., Sakai, K., Takasu, F. & Shigesada, N. 2000 Morphological plasticity in the coral *Porites sillimaniani* and its adaptive significance. *Bull. Mar. Sci.* **66**, 225–239.
- Rosner, B. 1983 Percentage points for a generalized ESD many-outlier procedure. *Technometrics* **25**, 165–172. (doi:10.2307/1268549)
- Shaish, L., Abelson, A. & Rinkevich, B. 2007 How plastic can phenotypic plasticity be? The branching coral *Stylophora pistillata* as a model system. *PLoS ONE* **2**, e644. (doi:10.1371/journal.pone.0000644)
- Succi, S. 2001 *The lattice Boltzmann equation: for fluid dynamics and beyond*. Oxford, UK: Oxford University Press.
- Todd, P. A. 2008 Morphological plasticity in scleractinian corals. *Biol. Rev.* **83**, 315–337. (doi:10.1111/j.1469-185X.2008.00045.x)
- Todd, P. A., Sidle, R. C. & Lewin-Koh, N. J. I. 2004 An aquarium experiment for identifying the physical factors inducing morphological change in two massive scleractinian corals. *Biol. Rev.* **83**, 315–337.
- Vermeij, M. J. A., Diekmann, O. E. & Bak, R. P. M. 2003 A new species of scleractinian coral (Cnidaria, Anthozoa), *Madracis carmabi* n. sp. from the Caribbean. *Bull. Mar. Sci.* **73**, 679–684.
- Veron, J. E. N. 1995 *Corals in space and time: the biogeography and evolution of the Scleractinia*. Sydney, Australia: UNSW Press.
- Wallace, C. C. 1999 Staghorn corals of the world: a revision of the genus *Acropora*. Collingwood, Australia: CSIRO.
- Wells, J. W. 1973*a* New and old scleractinian corals from Jamaica. *Bull. Mar. Sci.* **23**, 116–155.
- Wells, J. W. 1973*b* Two new hermatypic corals from the West Indies. *Bull. Mar. Sci.* **23**, 925–932.
- Willis, B. L. 1985 Phenotypic plasticity versus phenotypic stability in the reef corals *Turbinaria mesenteria* and *Pavona Cactus*. *Proc. of the Fifth Int. Coral Reef Congress* **4**, 107–112.